(11)

ARI RR-92

aerodyne research, inc.

GROWTH OF CARBON PARTICLES IN ROCKET EXHAUST

Final Scientific Report

by

David M. Mann

September 1, 1973 - September 30, 1976

Prepared Under

Contract No. F44620-74-C-0005

For The

AIR FORCE OFFICE OF SCIENTIFIC RESEARCH
Bolling Air Force Base, D.C. 20332

bedford research park, crosby drive, bedford, massachusetts 01730 (617) 275-9400

AIR FORCE OFFICE OF SCIENTIFIC RESEARCH (AFSC)
NOTICE OF TRANSMITTAL TO DDC
This technical report has been reviewed and is
approved for public release IAW AFR 190-12 (7b).
Distribution is unlimited.
A. D. BLOSE
Technical Information Officer

(18) AFOSR (19) TR-76-1423

(14) ARI-RR-92

(6) GROWTH OF CARBON PARTICLES IN ROCKET EXHUAST.

(9) Final Scientific Report. 1 Sep 73 - 30 Sep 76,

by

(10) David M. Mann

AERODYNE RESEARCH, INC.

Bedford Research Park, Crosby Drive
Bedford, Massachusetts

(11) Nov 76

(12) 36 p.

Prepared Under
(15) Contract No. F44620-74-C-0005

(16) 9711

For The

(17) 01

AIR FORCE OFFICE OF SCIENTIFIC RESEARCH
Bolling Air Force Base, D.C. 20332

September 1, 1973 - September 30, 1976

390112

ABSTRACT

The specific approach taken in this work was to study particle formation in a cooling jet of carbon vapor diluted by an inert carrier gas. Vapor was produced by the evaporation of a resistance heated graphite tube. The carbon vapor, mixed with carrier gas, flowed into a light scattering chamber where spectroscopic measurements were used to monitor concentrations of molecular species. Particles were also collected for electron microscopy. An initial reaction leading to particle formation was identified as $C_2 + C_3 \rightarrow C_5$ with a gas kinetic rate. Particulates were found to be spherical, of approximately equal diameter and frequently chained in the manner of hydrocarbon soot.

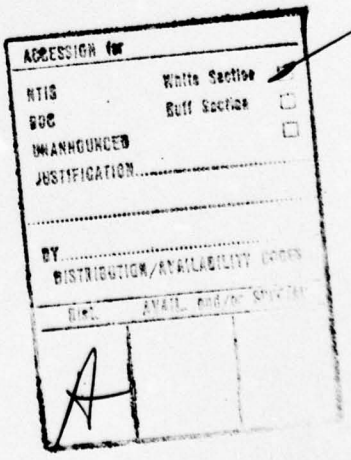

TABLE OF CONTENTS

LIST OF ILLUSTRATION

1. INTRODUCTION

The formation of particulates is an important component of most high temperature combustion processes. In general, the processes leading to the formation of observable particulates (e.g., particle sizes greater than a few microns) are obscured by a complex set of combustion mechanisms. As a result, there is little known about the formation of particulates from high temperature species (e.g., carbon, alumina, etc.). In the research described in succeeding sections of this report, data has been obtained on the formation of carbon particles by condensation of carbon vapor in a flowing inert gas system. From these data, it has been possible to identify a probable mechanism and determine the rate constant for the first-step reaction in the particle formation chain. In addition, electron micrographs of "old" particles have revealed at least a strong physical relationship between particulates formed from the condensation of pure carbon vapor and those formed hydrocarbon combustion. The final effort in this program has been directed toward the development of a molecular beam sampling system employing mass spectrometric detection of carbon species. At the termination of the present contract, this system was not yet operational.

The following sections include: a description of the experimental apparatus and measurement technique (Section 2); a presentation of the observed atomic, molecular, and particulate species behavior (Section 3); a discussion of these data from the standpoint of carbon particulate formation (Section 4); in addition, observations of the combustion of C_3 will be presented (Section 5).

2. APPARATUS AND MEASUREMENTS

2.1 Carbon Furnace and Flow System

The heart of the experimental apparatus is the carbon vapor source and associated flow system shown in Figure 1. Carbon vapor is produced by resistively heating a graphite tube (Ultra Carbon grade F4F) supported in the center of the furnace by clamping between graphite blocks. Power is supplied to the furnace via copper bus-bars from a high current, low voltage variac – controlled AC power supply. Maximum input power is 12 kw (12V, 1000A). Water cooling is employed in the entire assembly with the main heat loading produced at the upper and lower graphite blocks. Radiation losses from the tube walls are reduced by concentric tantalum heat shields which are, in turn, surrounded by graphite felt insulation to reduce conduction losses. Furnace temperature is measured by an optical pyrometer sighted onto the heated tube wall. As shown in Figure 1, the distance from furnace exit to optical axis is 5 cm. In order to observe changes with distance, modifications were made to the system to give 2, 5, and 15 cm distances. The 2 cm distance was achieved by modifying the upper graphite support so that it extended into the scattering chamber. A 10 cm spacer between the furnace and scattering chamber gave a 15 cm total distance.

A carrier gas, usually argon, is admitted into the lower end of the heated tube through holes in the lower graphite support. The argon mixes with the carbon vapor subliming off of the tube wall. The argon/vapor mixture exits the tube into the upper section where optical and probe sampling measurements are performed. Total argon flow rates are from 1 to 100 cm^3/sec (STP) as measured by standard rotameters. Flow is maintained by exhausting the chamber with a 1000 ℓ/m mechanical pump.

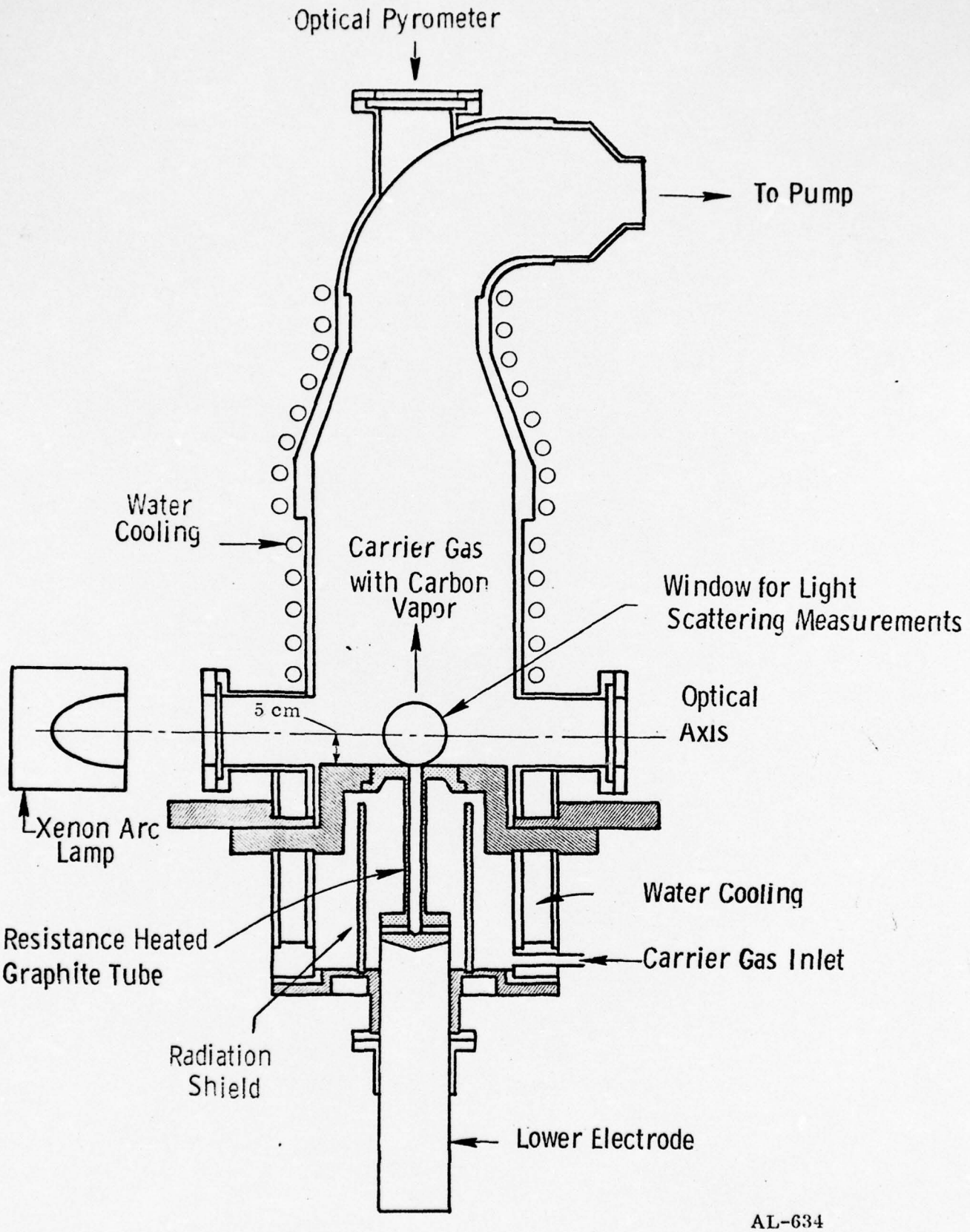

Figure 1 - Carbon Particle Apparatus

2.2 Molecular Beam Mass Spectrometer

The molecular beam mass spectrometer provides the most balanced molecular species diagnostic tool currently available. It is able to monitor all molecular species, function in the temperature/pressure range of interest to high temperature condensation, provide good spatial resolution, and monitor without major disturbance to the thermodynamic state of the system. The apparatus is shown in Figures 2 and 3. The source gas expands as a free jet through the inlet nozzle orfice into the first chamber ($p \sim 10^{-4}$ torr). The skimmer allows only the central core to further expand into the collimating chamber ($\sim 10^{-6}$ torr) and hence, into the mass spectrometer. The mass spectrometer detector generates a signal proportional to the species density in the beam. By modulating the beam of gas before detection, it is possible to substantially improve the detection signal-to-noise ratio.

"Freezing" of reacting species at near their actual presampled concentrations is accomplished by the rapid temperature drop upon expansion through the inlet nozzle. For a source at 2000^{o}K, 1.0 atmosphere pressure expanding through a 0.10 mm opening, the quenching time is about 1 μsec.

Inlet nozzle diameter is determined by the requirement that the nozzle lip not perturb the central gas flow and the need to avoid nozzle clogging by large particles. These requirements will be satisfied for diameter to mean-free-path (D/λ) ratios greater than 100 or for operating conditions by D = 0.13 mm. For so large an orifice, it is necessary to use a 16 in. diffusion pump in the first chamber in order to hold the pressure to 1×10^{-4} torr and ensure a free jet expansion with no strong shock influence.

The beam enters the final, mass spectrometer chamber through a collimating orifice and remotely controlled valve. (Separation of the mass spectrometer from the rest of the apparatus is desirable to control contamination.) For an inlet nozzle-to-mass spectrometer ionizer distance of 30 cm and an ionizer orfice of 10^{-2} cm^2, there will be a species flux of 5×10^{14}/sec in the ionizer.

The mass spectrometer shown in Figure 2 is a quadrupole type using a molecular beam ionizer. This type of ionizer gives high ionization efficiency (10^{-2}) by allowing the spectrometer to be positioned parallel to the flow. Protection from contamination

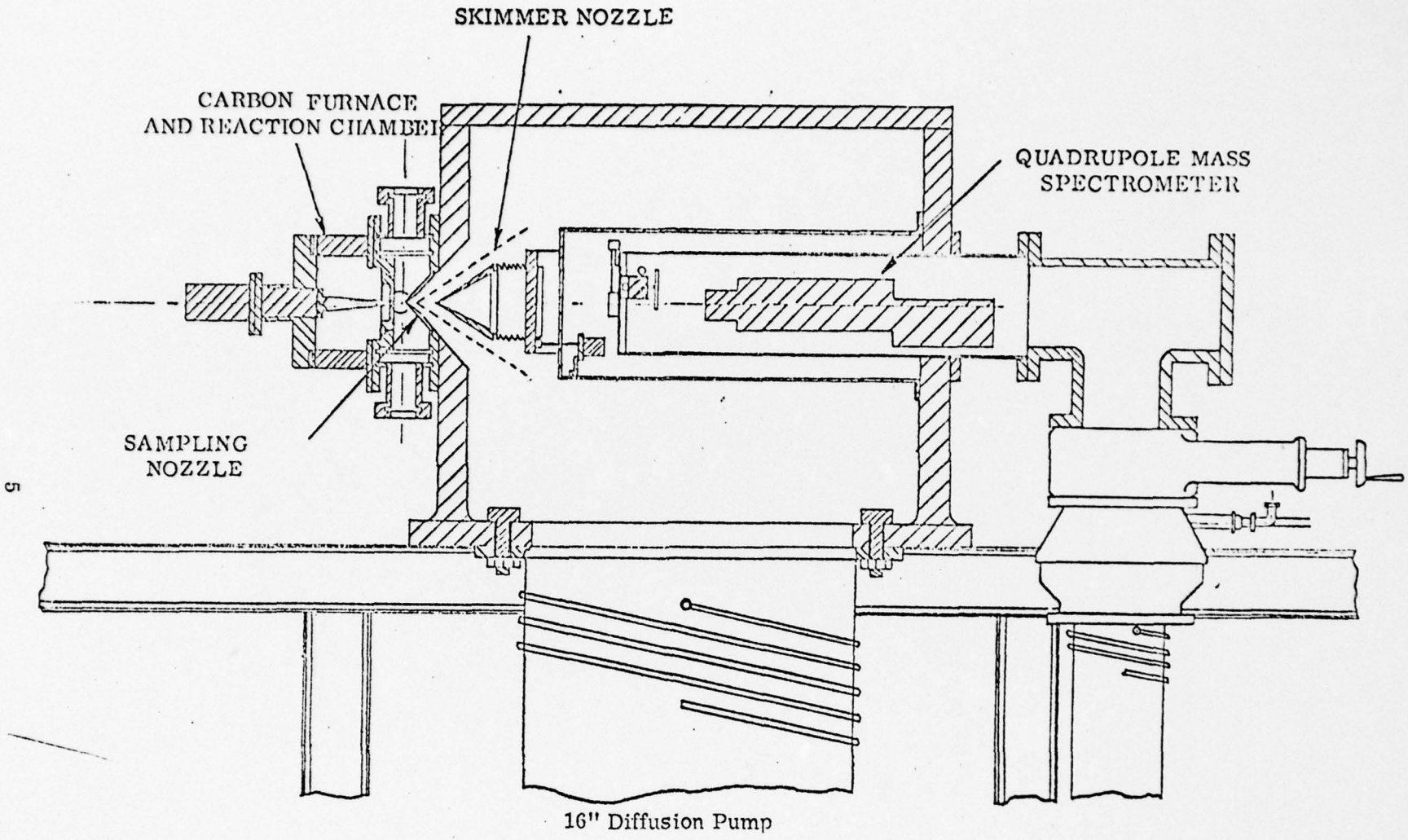

Figure 2 - Furnace and Mass Spectrometer Section View

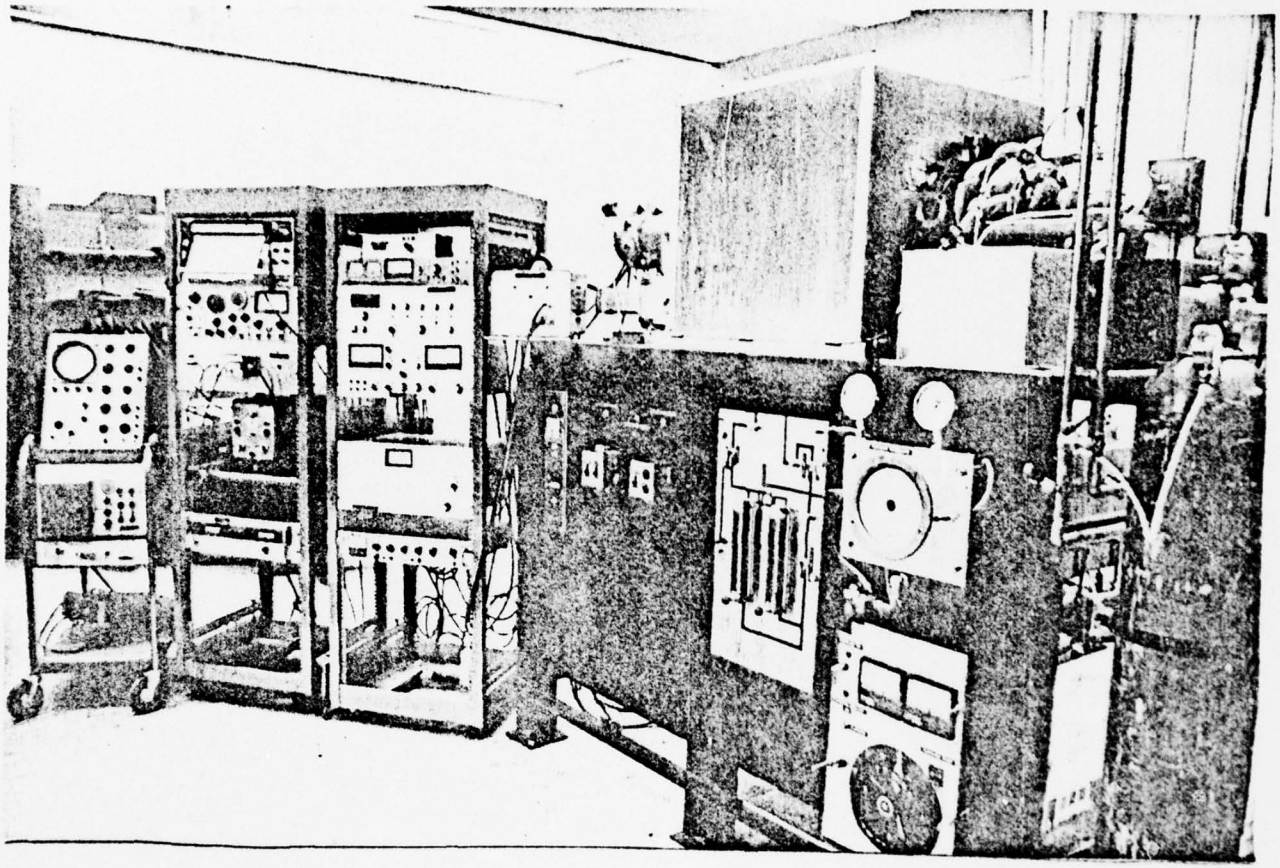

Figure 3 - Molecular Beam Mass Spectrometer System - From Left to Right: Mass Spectrometer Controls, Vacum System, and Carbon Furnace (mounted on right side of vacuum chamber)

by condensable species can be added by placing a liquid nitrogen cooled baffle around the ionizer, but this should not be required with the well collimated beam described here. Molecules entering the ionizer are ionized with an efficiency (η_{ion}) of 1%. They are drawn out of the ionizer by an electric field and into the quadrupole mass spectrometer. By varying the AC and DC voltages supplied to the quadrupole it is possible to ensure that only ions of a given mass-to-charge ratio can completely traverse the quadrupole. Ions are detected using an electron multiplier in which the detected ion current is multiplied by typically 10^5.

The major limitation to the quadrupole detector is the presence of background species in the detector chamber. The effect of these background species ($3 \times 10^9/cm^3$ at 10^{-7} torr) can be considerably reduced by chopping, or modulating the molecular beam before it reaches the ionizer. The background species, since they are not modulated, provide a DC level which is removed by AC detection at the chopping frequency. Unfortunately, their effect is not completely eliminated, since there are Fourier components of the natural oscillations of the background gas in the chamber which extend into the range of the modulating frequency. However, a reduction on the order of 1/250 is possible for the system described here.

2.3 Measurements

2.3.1 Spectroscopy

Molecular carbon species in the flowing gas stream are monitored by spectroscopic means by detection of either the light emitted from thermally excited species or resonantly scattered from cooler species. Figure 4 shows the detection system used for scattering measurements. A 500w, Xe light source is focused through a chopper wheel and passes into the chamber. Light scattered at 90^o to the incident beam is focused onto the entrance slit of a 0.25m scanning monochromator. The monochromator output is detected using an S-20 photomultiplier whose signal, after passing through a lock-in amplifier at the chopper frequency, is displayed on a chart recorder. This system suppresses the strong emission from the hot furnace. For studies of emission, the light source was not used and the chopper was placed in the optical path between the chamber and monochromator.

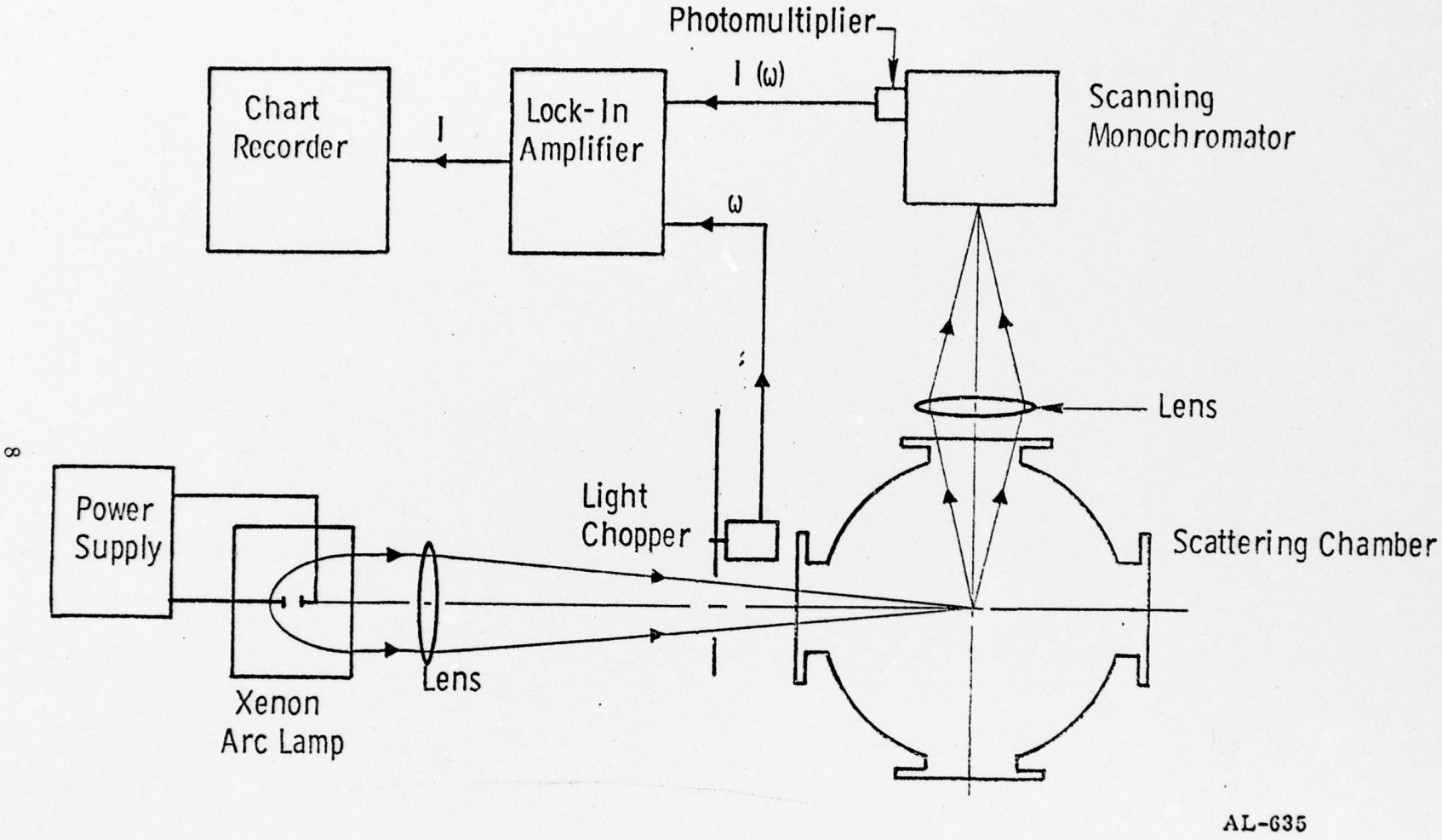

Figure 4 - Carbon Particle Formation Studies, Light Scattering and Detection System Schematic

A pulsed system was used to detect atomic carbon species whose resonant scattering is the vacuum ultraviolet. A pulsed discharge lamp using a MgF_2 window was attached to one port of the scattering chamber. At 90^o to the light source, a second MgF_2 window and MgF_2 lens were used to focus the scattered light onto a 0.3m evacuable monochromator. Both solar-blind and Suprasil quartz enveloped S-20 photomultipliers were used. Phototube signals were displayed on a fast oscilloscope. In operation, the monochromator and optical path were purged with nitrogen to remove oxygen absorption.

2.3.2 Particle Collection

Particles were collected from the scattering chamber for electron microscopy. Because of the high temperatures in the jet, special carbon film on tungsten electron microscope grids were used. Grids were supported on a stainless steel probe equipped with a rotatable shutter. The probe was inserted into the flow through a port on the scattering chamber. Electron micrographs of the collected particles were taken on a transmission electron microscope having an ultimate resolution of 1.5 nm. Unfortunately, the carbon films used to collect particles severely degraded the resolution to 5 nm.

2.3.3 Mass Spectrometry

As was mentioned earlier, the mass spectrometer system did not become operational before the end of this contract. The major problem areas were difficulties in fabrication of the vacuum system and nozzle assemblies and continuing instrumental problems with the mass spectrometer itself. While the mechanical problems were finally overcome the instrumental ones persisted and the complete mass spectrometer was returned to the manufacturer for repair. The main problem was one of sensitivity and signal-to-noise ratio. With 40 torr pressure of argon in the carbon furnace, the noise level limited the minimum signal to 10^{-3} of the argon signal. This minimum signal level corresponds to 4×10^{-2} torr of carbon as the minimum detectable. Referring to Figure 5, this requires a furnace temperature in excess of 2700^oK for C_3 and 3000^oK for C_2. Operation at these temperatures for extended periods of time was not feasible due to rapid degradation

of the graphite electrode. The measured system sensitivity corresponded to approximately 10^{-3} of the expected value. Further, problems of mass spectrometer stability and poor mass resolution pointed to the need for equipment overhaul before the experimental goals could be attained.

3. OBSERVATIONS

3.1 Gas Phase Species

Mass spectrometric studies[1] have shown that the principal constituent of equilibrium carbon vapor is C_3 with lesser amounts of C and C_2 species followed by traces of higher carbon molecules. The vapor pressures of these species at temperatures from 1800 to 3000°K are shown in Figure 5.

The carbon molecules C_2 and C_3 have near resonant or resonant transitions in the visible portion of the spectrum. For C_2, strong emission is observed in many carbon/hydrocarbon environments from the $d\,^3\Pi - a\,^3\Pi$ Swan bands with 0, 0 band at 516.5 nm. Strictly speaking, this is not a resonant transaction, since the $a\,^3\Pi$ state is not the C_2 ground state. However, the $a\,^3\Pi$ state is only 715 cm^{-1} above the ground state and has an appreciable population in most situations. (C_2 ($a\,^3\Pi$)/C_2 ($x\,^1\Pi$) = 0.1 at 450°K.) The comet head or 405 nm bands characterize emission from the C_3 molecule. This is a complex band system extending from about 390 to 430 nm which is produced by the overlap of many individual vibronic bands.

Typical fluorescence spectra obtained 2 and 15 cm above the furnace exit are shown in the upper trace of Figure 6. Fluorescence is observed from the $\Delta V = -1, 0, 1$ sequences of the C_2 Swan bands and from the C_3 comet-head bands which show a main peak at 405 nm and a secondary bump at 430 nm. Also present in the spectrum is the sodium doublet at 589 nm and an unidentified line at 422.5 nm. Both of these latter features are apparently produced by impurities and disappear as the electrode is heated.

At 2 cm above the furnace exit, C_2 and C_3 fluorescent intensities increase with temperature following the expected equilibrium vapor pressure curves of Figure 5. This behavior is shown in Figure 7. The large scatter apparent in the data is due to the ± 10°K uncertaintly in setting the furnace temperature as monitored by an optical pyrometer.

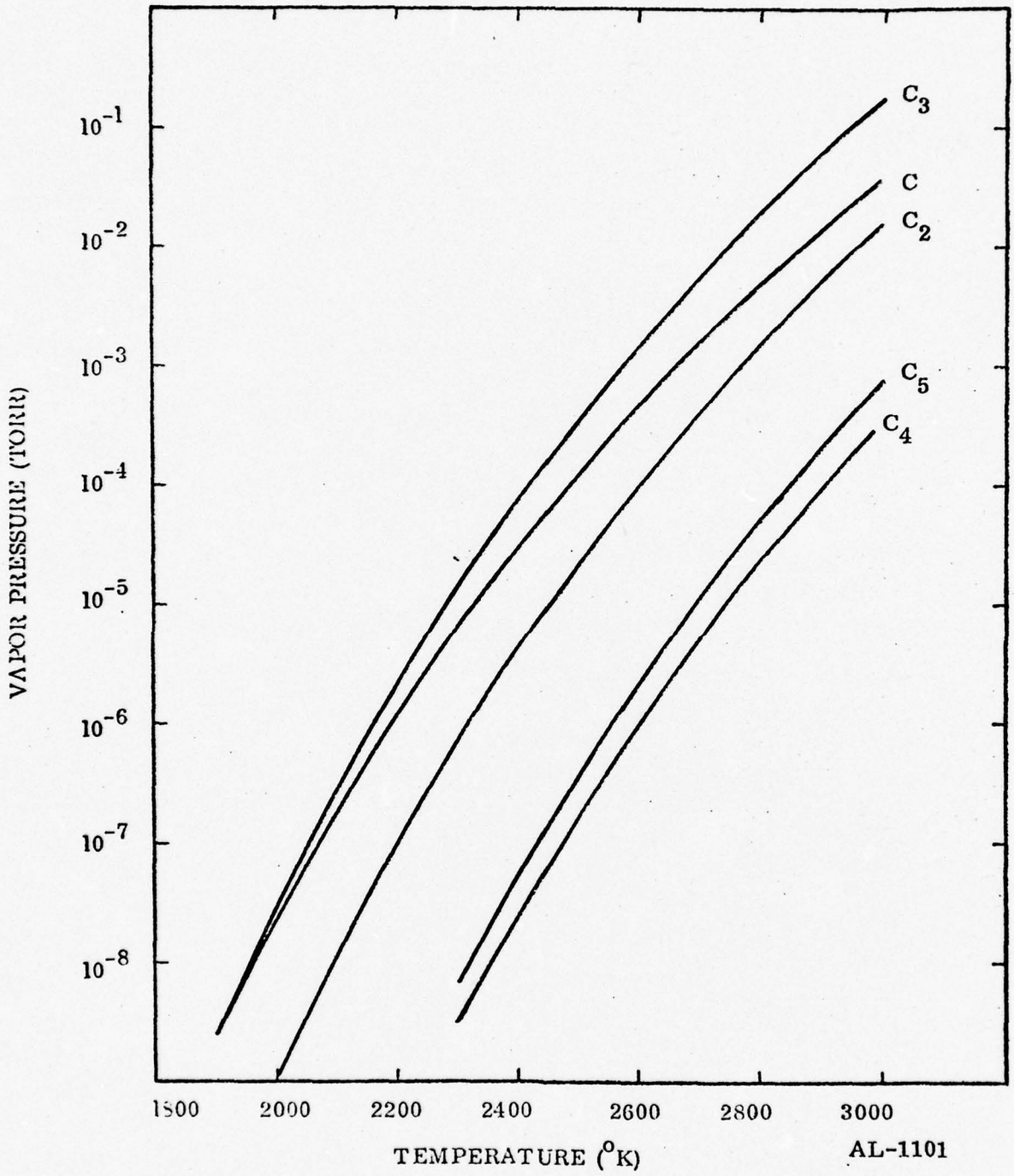

Figure 5 - Vapor Pressure of Major Carbon Species as Determined by Mass Spectrometry (Ref.(1))

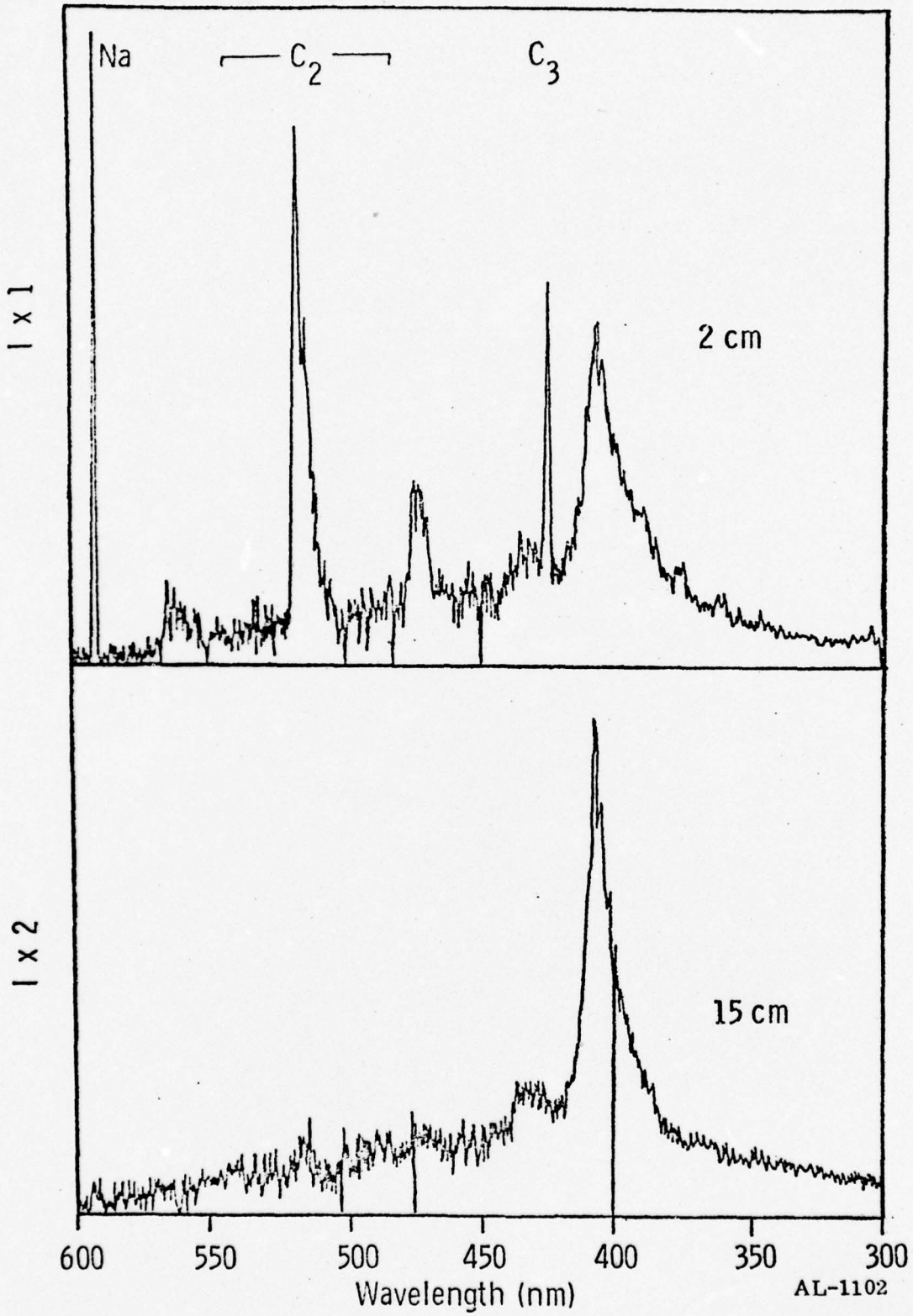

Figure 6 - Fluorescence Spectra at 2 and 15 cm From Furnace Exit

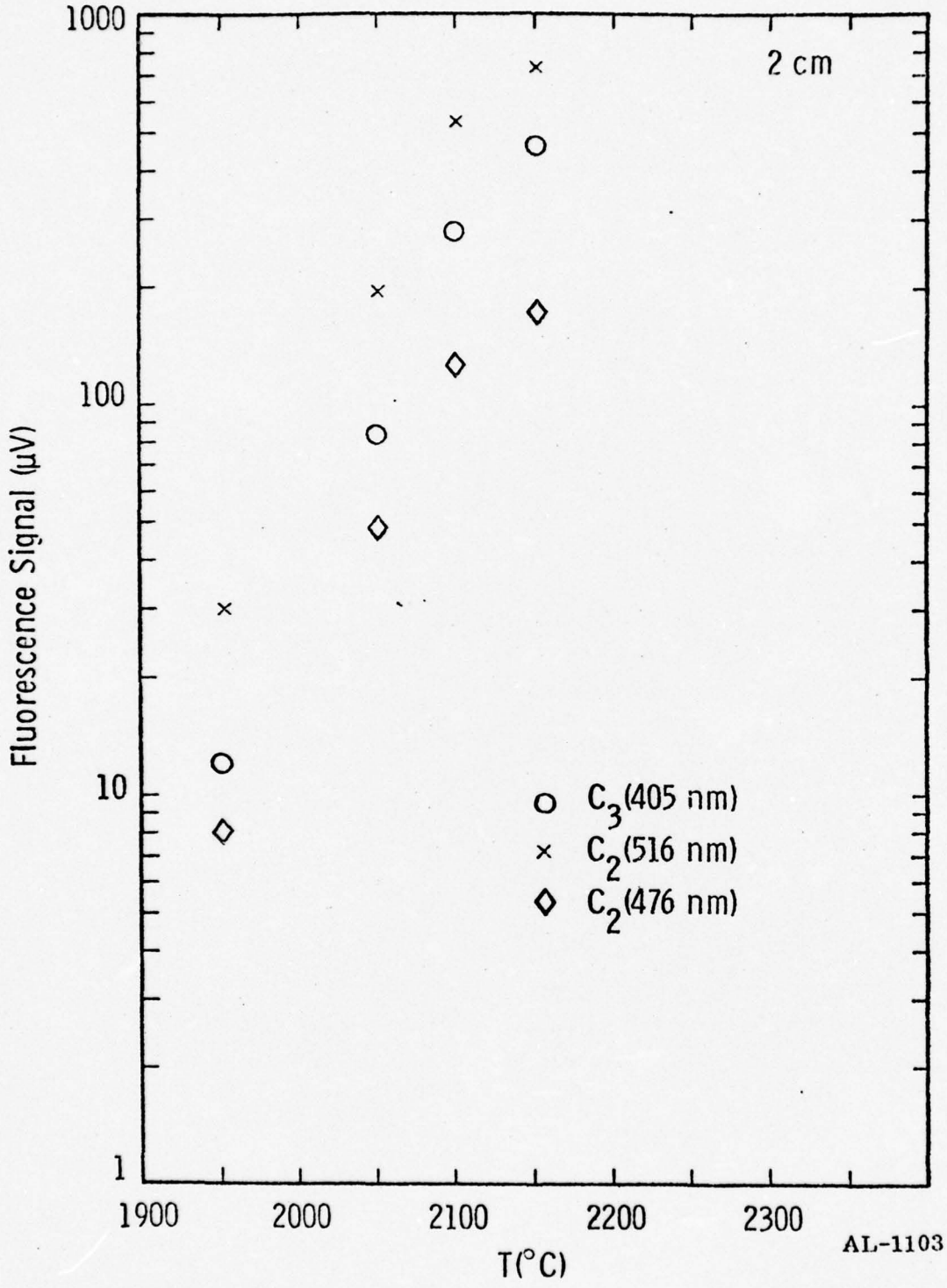

Figure 7 - Fluorescence Signal versus Furnace Temperature

Species concentrations were found to be uniform across the furnace exit. This was determined by scanning a 2 mm segment of the input light beam over the 1 cm diameter jet. No change in fluorescent intensity was observed until the beam intersected the edge of the jet.

Relative concentrations of C_2 and C_3 were observed to vary rapidly with downstream distance as illustrated by the spectra of Figure 6. Both spectra were taken at a furnace temperature of 2200°C with 39 cm^3/sec (STP) argon flow at 40 torr total pressure. These conditions correspond to a jet velocity of 84.8 m/sec which gives a time difference of 1.56 msec between observations at the 2 and 15 cm distances.

At the 5 and 15 cm downstream distances, variation of relative species concentrations with temperature was observed to depart from furnace equilibrium value. By 15 cm, the effect became quite pronounced and appeared as illustrated by the spectra in Figure 8. These spectra, obtained at 39 cm^3/sec (STP) flow and 40 torr, show a rapid decrease in C_2 concentration at higher temperatures. Figure 9 gives the observed temperature dependence of C_2 and C_3 fluorescence intensities over the temperature range of 1950 to 2250°C at 15 cm.

Experiments designed to follow carbon atom concentrations proved disappointing due to difficulties with the pulsed light source. Data were obtained at 2 cm above the furnace indicating the presence of carbon atoms as indicated by observation of the 193.1 nm ($^1D - {}^1P$) transition. However, further experiments showed no C-atom emission. An examination of the pulsed light source revealed substantial window opacity which probably severely attenuated the VUV output. The experiments will be repeated when a more suitable, preferably CW, light source can be obtained.

3.2 Particulates

As can be seen from Figures 6 and 8, there appears to be little or no continuum scattering background of the type which would be expected if particulates were present in the gas stream. Visibly, particulate scattering may be seen in the recirculation region surrounding the jet which at higher pressures and slower flows can mix with the central jet giving rise to the continuum scattering reported earlier.[2]

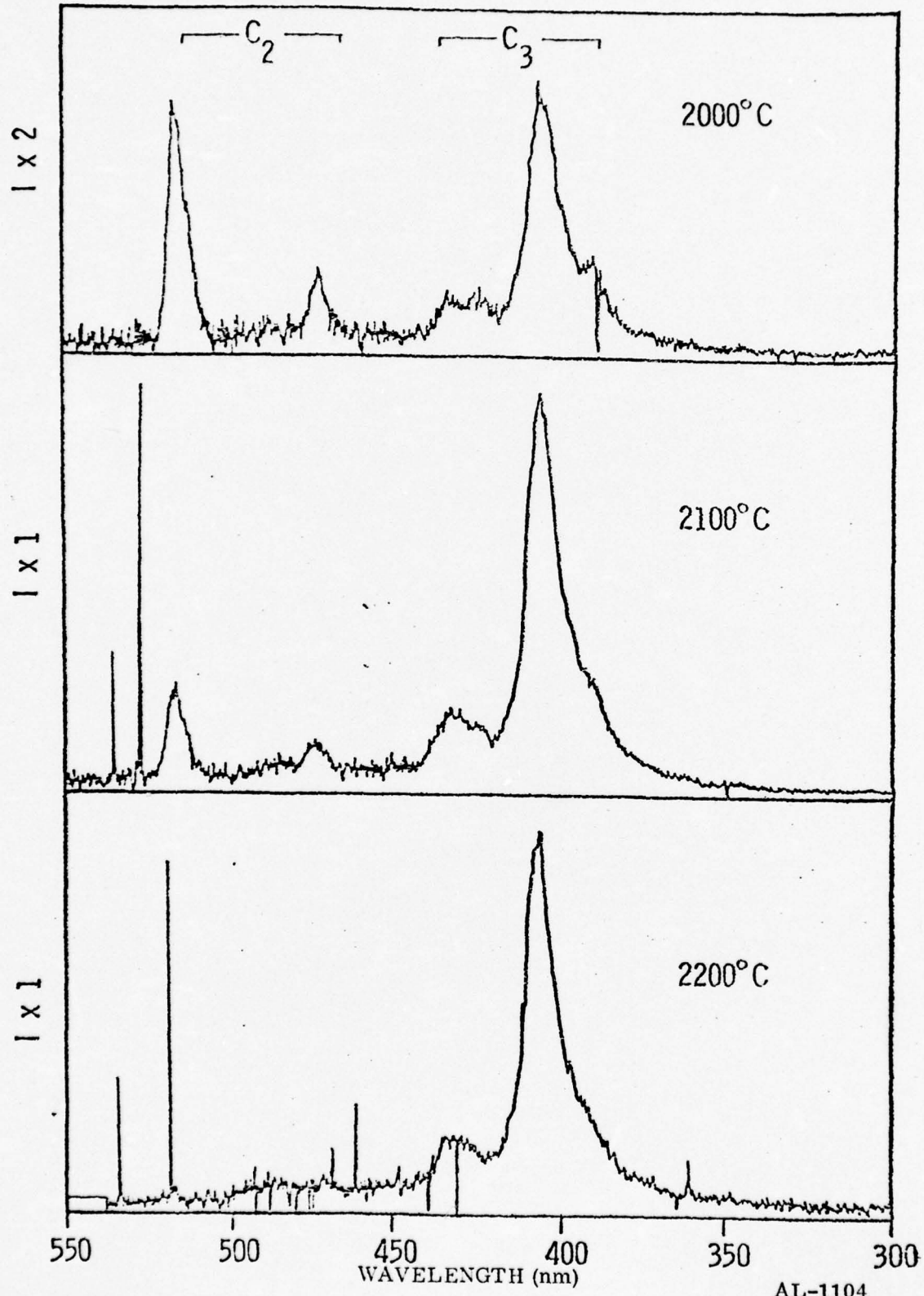

Figure 8 - Fluorescence Spectra versus Furnace Temperature at 15 cm From Furnace Exit

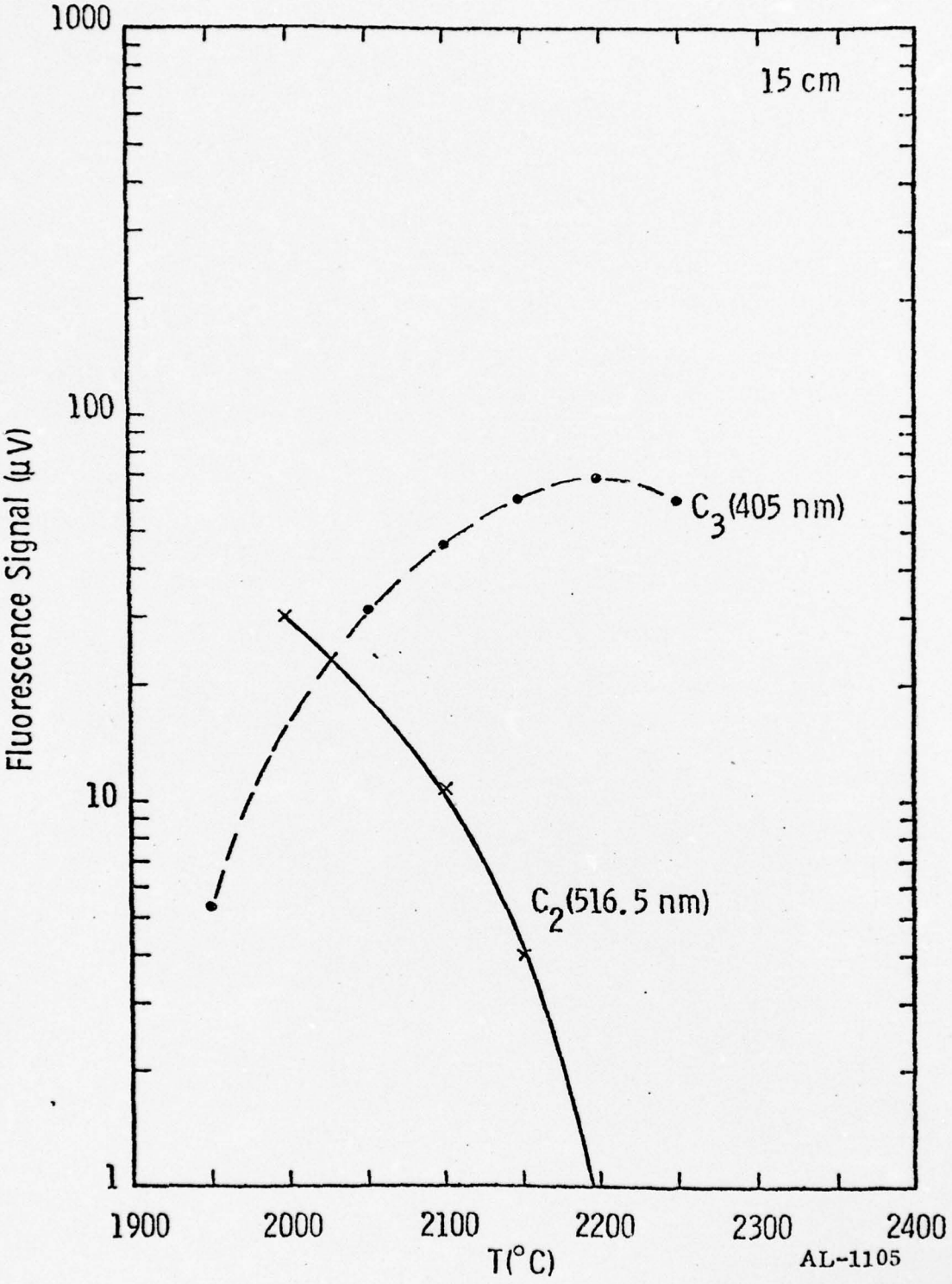

Figure 9 - Fluorescence Signal versus Furnace Temperature

Attempts to collect samples of particulates from the jet were unsuccessful. Electron microscope pictures of grids exposed to the central jet at 2 and 15 cm distances showed no particulates. In the recirculation region, particulates were easily collected. Figure 10 shows an electron micrograph of single and multiple carbon particles obtained 5 cm above the furnance at 20 torr pressure and 2240^{o}C furnace temperature. The particles are spherical and of approximately equal diameter ($d \simeq 35$ nm). A break in the same grid allowed a large cluster to form as shown in Figure 11. This structure was apparently produced by agglomeration on the grid surface and, again, is composed of equal diameter particles ($d \simeq 35$ nm). There is some branching evident indicating the capture of multiple particle groups from the gas stream. At 15 cm, downstream with higher pressure (40 torr) and lower temperature (2050^{o}C), major clustering takes place in the gas stream as well as on the grid surface. Figure 12 shows the complicated structuring possible at longer times in the cooler environment. It is interesting to note that the individual particles still have an approximately constant diameter of 35 to 40 nm.

AL-1106

Figure 10 - Particles Collected 5 cm From Furnace at 20 torr (250,000 magnification)

AL-1107

Figure 11 - Particle Agglomeration on Edge of Grid. Collected at 20 torr, 5 cm From Furnace (100,000 magnification)

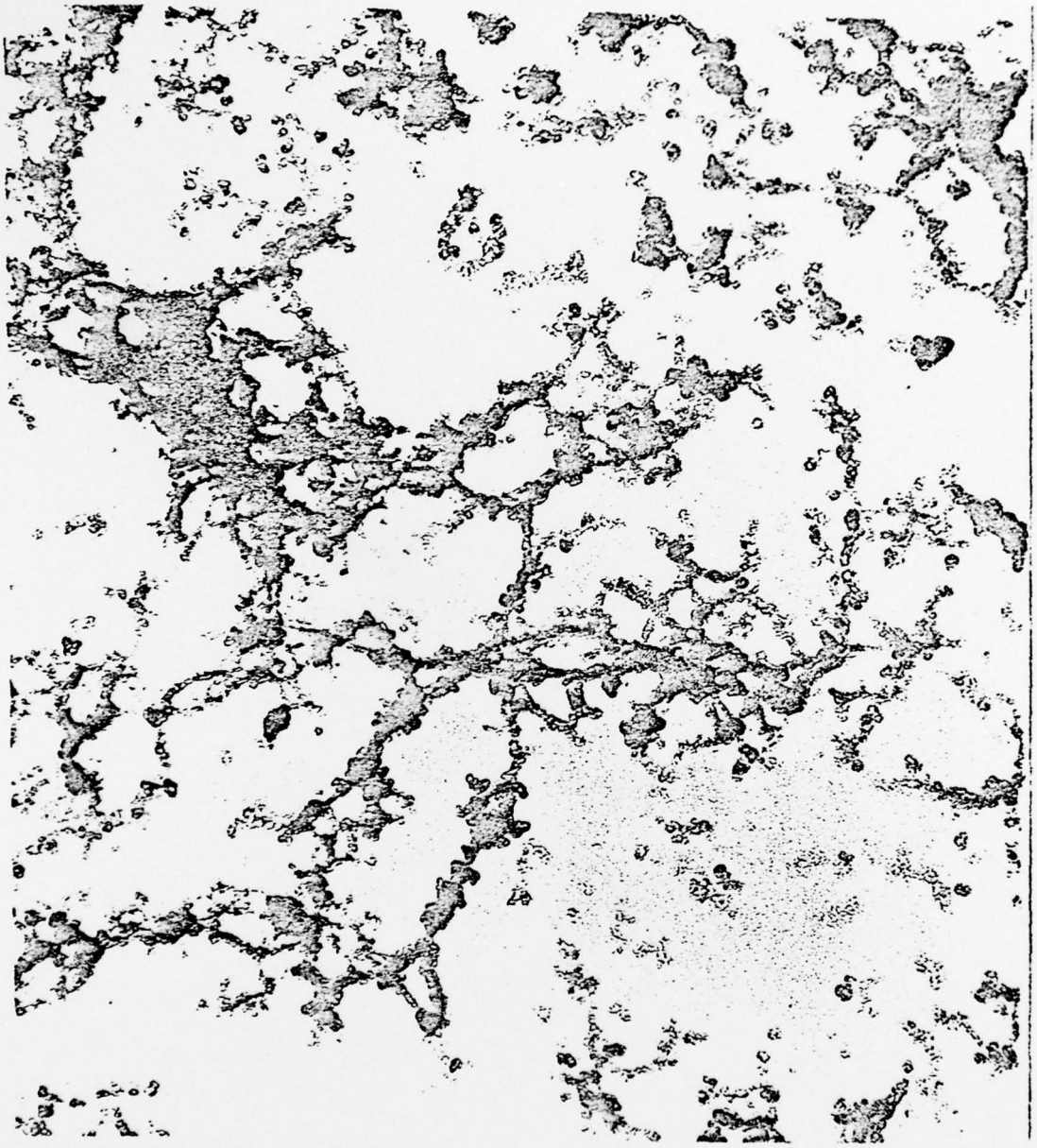

AL-1108

Figure 12 - Carbon Particles Collected at 40 torr, 15 cm From Furnace (25,000 magnification)

4. DISCUSSION

4.1 Formation of Carbon Nuclei

Traditional particle formation theories employ the concept of a thermodynamically stable "critical nucleus" upon which further particle growth can take place. This critical nucleus is the smallest size particle which can be held together by the surface tension of the bulk material. While this method has had some success with low temperature materials, e.g., water and alcohol, it is not necessarily valid for high melting point materials. In the case of carbon,[3] the predicted "critical nucleus" is the polyatomic molecule C_5. Therefore, it seems more appropriate to try to analyze the formation of particles from carbon in terms of a series of reactions leading from gas phase species to particles. Three possible reaction schemes are possible:

Three-body Recombination

$$C_x + C_y + M \rightarrow C_{x+n} + C_{y-n} + M \quad , \tag{1}$$

Bimolecular Exchange

$$C_x + C_y \rightarrow C_{x+n} + C_{y-n} \quad , \text{ and} \tag{2}$$

Bimolecular Coalescence

$$C_x + C_y \rightarrow C_{x+y} \quad . \tag{3}$$

In the first process, the total species concentration may or may not decrease depending on the value of n.

The most dramatic feature of the data presented in Subsection 3.1 is the rapid variation of C_2 intensity with distance and temperature. Both of these features (i.e., distance and temperature variation) must be manifestations of a reaction of the form

$$C_2 + C_x (+ M?) \xrightarrow{K} C_n (+ M?) \quad , \tag{4}$$

where there is the possibility of any of the three reaction schemes discussed above. From the decrease of C_2 intensity with distance at constant velocity, a characteristic reaction time, τ, defined as

$$\frac{1}{\tau} = \frac{1}{[C_2]} \frac{d[C_2]}{dt} = K[C_x] \tag{5}$$

may be obtained. The observed τ is between 0.3 and 0.5 msec. This reaction time is too short for three-body recombination and is only possible for the bimolecular exchange or coalescence reactions with C_3. That is, the reaction must be of the form

$$C_2 + C_3 \xrightarrow{K} \begin{cases} C_3 + C \\ \text{or} \\ C_5 \end{cases} \quad , \tag{6}$$

with a rate constant $K = 1/[C_3]\tau$ equal to the gas kinetic rate (3×10^{-10} cm^3/sec). The decrease in C_2 intensity with temperature at 15 cm downstream shown in Figure 7. also gives a rate constant equal to gas kinetic. If Eq. (5) is integrated to obtain the C_2 concentration at time t in terms of initial concentrations of C_2 and C_3, the result is

$$[C_2]_t = \frac{[C_2]_0 \delta \exp[-\delta Kt]}{[C_3]_0 - [C_2]_0 \exp[-\delta Kt]} \quad , \tag{7}$$

where $\delta = [C_3]_0 - [C_2]_0$. In the limit that $[C_3]_0 >> [C_2]_0$, approximately true in these experiments, it is possible by applying Eq. (7) twice to obtain the ratio of C_2 concentrations at two different temperatures, $T_1 + T_2$:

$$\frac{[C_2(T_1)]_t}{[C_2(T_2)]_t} = \frac{[C_2(T_1)]_0}{[C_2(T_2)]_0} \exp\left\{ -[\delta(T_1) - \delta(T_2)]\, Kt \right\} \quad . \tag{8}$$

Assuming that C_2 and C_3 concentrations are initially at their equilibrium values (cf. Figure 7) and the flow conditions appropriate to the data of Figure 9, the rate constant obtained from Eq. (8) is $K = 7 \times 10^{-10}$ cm^3/sec. Thus, the two observed phenomena are describable by the same reaction scheme and the reaction rate is approximately gas kinetic.

The above discussion has demonstrated that an early reaction in carbon particle formation is between C_2 and C_3. The product species was not detected. There are three pieces of evidence supporting the conclusion that the reaction is $C_2 + C_3 \rightarrow C_5$ instead of $C_4 + C$.

1) Recent studies of matrix isolated carbon species[4] have predicted a gas-phase transition of the C_4 molecule at about 520 nm; such a transition was not observed

2) Molecular orbital calculations[5] predict that carbon molecules with odd-numbers of atoms are more stable than their even-numbered neighbors.

3) C_2, C_3, C_4 and C_5 all have singlet ground states while the carbon atom ground state is a triplet. Thus, the only spin allowed formation route leading to $C_4 + C$ is via an exited state. The reaction would be spin allowed if it proceeded from the lowest excited state of C_2 ($a\,^3\Pi$).

4.2 Particles

Electron microscope pictures of particulates produced by the condensation of carbon (Figures 10, 11, and 12) show structures remarkably similar to those of soot particles from hydrocarbon combustion.[6] Even for very large chained structures, the basic particle appears to be spherical with a diameter of 35 to 45 nm. Since electron microscope resolution was limited to 5 nm, it was impossible to determine if the particles were amorphous or composed of still finer particles. The chain-like structures suggest that some, if not all, of the particles may possess significant amounts of electrical charge.[7]

5. OBSERVATIONS OF THE COMBUSTION OF C_3

Reactions between gaseous oxygen and carbon vapor have been reported using vapor cooled to room temperature.[8] In view of the substantial cooling and the absence of emission from C_3 species, it is probable that the reactions studied were between gaseous oxygen and microparticles of carbon. The carbon vapor source described in Subsection 2.1 provides the opportunity to study reactions using molecular carbon.

Oxygen was added to the argon/carbon vapor flow 5 cm above the jet through a pyrex tube inserted in place of the electron microscope grid probe. The result of O_2 addition was a bright green flame extending from the furnace exit. The lower trace of Figure 13 shows the emission from carbon vapor in the absence of added oxygen at 100 torr, 2200°C furnace temperature, and 86 cm^3/sec (STP) flow rate. Strong emission from C_3 and weaker amounts of C_2 is evident. Upon addition of 0.2 cm^3/sec (STP) O_2, the upper spectrum in Figure 13 was obtained. There has been a 50% consumption of C_3 accompanied by a 300-fold increase in C_2 emission. Also evident is an increase in intensity from those Swan bands with $v' = 1$, suggesting that the combustion proceeds by the previously proposed mechanism,[8]

$$C_3 + O_2 \rightarrow C_2^* + CO_2 \quad ,$$

but with preferential excitation of $v' = 1$.

These observations indicate that C_3 emission probably is produced during combustion in a fuel rich region of a reaction zone, and in the presence of excess oxygen, C_3 is rapidly consumed by the reaction above.

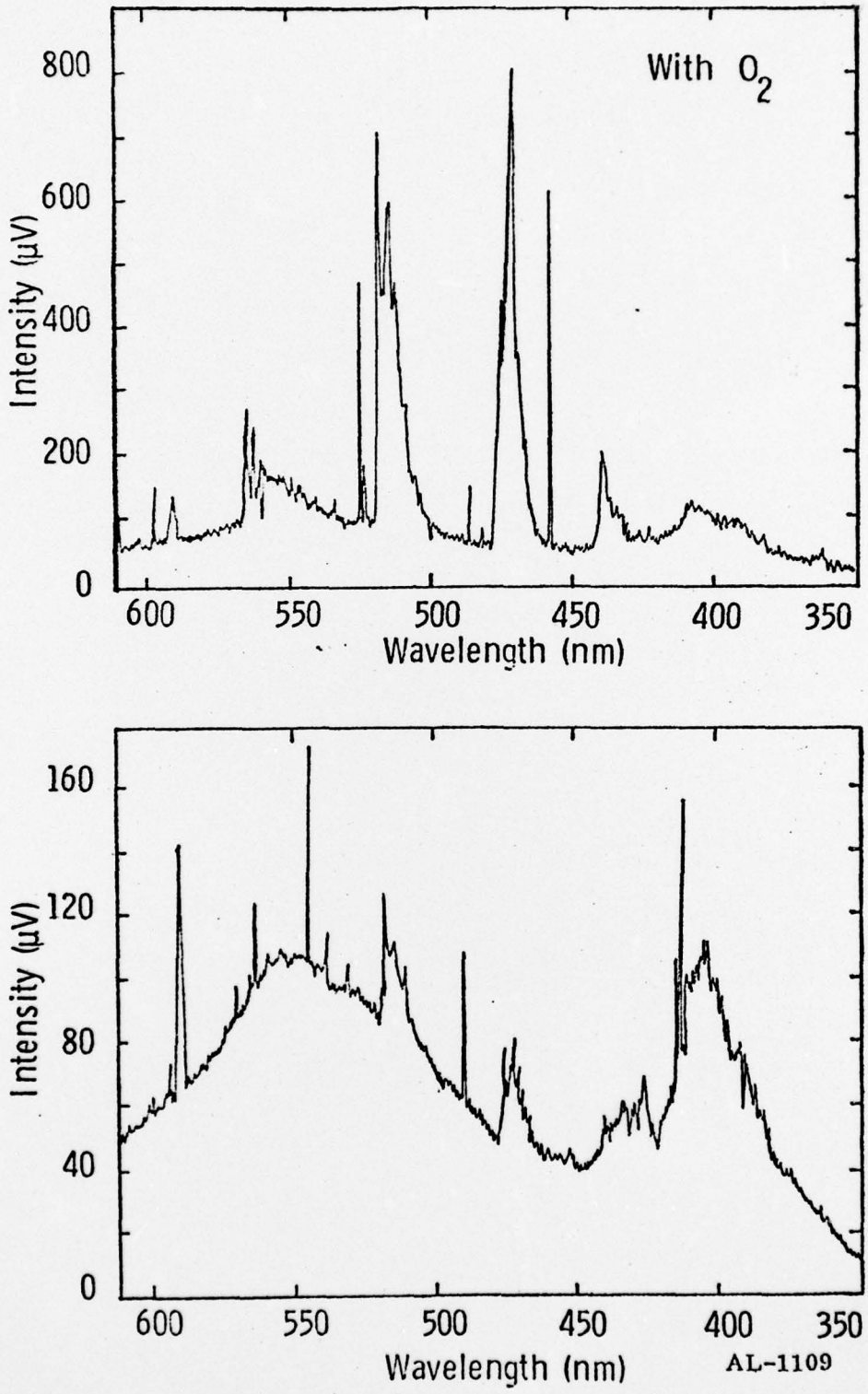

Figure 13 - Emission From Carbon Vapor With and Without Added Oxygen

6. ACKNOWLEDGMENTS

The author would like to acknowledge the advice and assistance of Prof. J. Howard and Dr. G. Prado of MIT in making the electron microscope measurements. The vacuum monochromator and solar blind photomultiplier were obtained on loan from the Air Force Geophysics Laboratory through Dr. D. Paulsen. The able assistance of Mr. R. Brown and Mr. S. Kallelis during the course of these experiments is greatly appreciated.

7. REFERENCES

1. J. Drowart, R.D. Burns, G. DeMaria, and M.G. Inghram, "Mass Spectrometric Study of Carbon Vapor," J.Chem.Phys. 31, 1131 (1959).
2. D.M. Mann, "Growth of Carbon Particles: Interim Scientific Report," AFOSR-TR- 74-1893 (October 1974).
3. D.E. Jensen, "Prediction of Soot Formation Rates: A New Approach," Proc. Roy. Soc. Section A (1974)
4. W.R.M. Graham, K.I. Dismuke, and W. Weltner, Jr., "The C_4 Molecule," (preprint)
5. K.S. Pitzer and E. Clementi, "Large Molecules in Carbon Vapor," J. Am. Chem. Soc. 81, 4477 (1959).
6. A.G. Gaydon and H.G. Wolfhard, Flames: Their Structure, Radiation, and Temperature, Chapman and Hall, London (1970).
7. J. Howard, "On the Mechanism of Carbon Formation in Flames," Proc. 12th Symposium on Combustion (1968)
8. M.I. Savadatti and H.P. Broida, "Spectral Study of Flames of Carbon Vapor at Low Pressure," J. Chem. Phys. 45, 2390 (1966).

8. REPORTS AND PUBLICATIONS

(Authored by D.M. Mann)

Reports

"Growth of Carbon Particles, Interim Scientific Report," ARI-RR-57 (October 1974)

"Growth of Carbon Particles, Interim Scientific Report," ARI-RR-72 (October 1975)

Publications

"Carbon Particle Formation by Condensation of Carbon Vapor in a Flowing Inert Gas," Bull. Am. Phys. Soc. 21, 13 (1976)

"A Molecular Carbon Vapor Source for Flowing Systems," Rev. Sci. Instrum., Vol. 47, No. 11, November 1976

"A Possile First Step in Carbon Particle Formation: $C_2 + C_3$," ARI-RR-75, Submitted to J. App. Phys.

"Chemiluminescence From C_2 Produced by C_3 Oxidation," Submitted to Chem. Phys. Lett.

UNCLASSIFIED

SECURITY CLASSIFICATION OF THIS PAGE (When Data Entered)

REPORT DOCUMENTATION PAGE	READ INSTRUCTIONS BEFORE COMPLETING FORM
1. REPORT NUMBER: AFOSR - TR - 76 - 1423	2. GOVT ACCESSION NO. / 3. RECIPIENT'S CATALOG NUMBER
4. TITLE (and Subtitle): GROWTH OF CARBON PARTICLES IN ROCKET EXHAUST	5. TYPE OF REPORT & PERIOD COVERED: Final Scientific Report 9/1/73 - 9/30/76
	6. PERFORMING ORG. REPORT NUMBER: ARI-RR-92
7. AUTHOR(s): David M. Mann	8. CONTRACT OR GRANT NUMBER(s): F44620-74-C-0005
9. PERFORMING ORGANIZATION NAME AND ADDRESS: AERODYNE RESEARCH, INC. Bedford Research Park, Crosby Drive Bedford, MA 01730	10. PROGRAM ELEMENT, PROJECT, TASK AREA & WORK UNIT NUMBERS: 681308 9711-01 61102F
11. CONTROLLING OFFICE NAME AND ADDRESS: AIR FORCE OFFICE OF SCIENTIFIC RESEARCH/NA Bldg. 410 Bolling Air Force Base, D.C. 20332	12. REPORT DATE: November 1976
	13. NUMBER OF PAGES: 34
14. MONITORING AGENCY NAME & ADDRESS (if different from Controlling Office)	15. SECURITY CLASS. (of this report): UNCLASSIFIED
	15a. DECLASSIFICATION/DOWNGRADING SCHEDULE

16. DISTRIBUTION STATEMENT (of this Report)

Approved for public release; distribution unlimited

17. DISTRIBUTION STATEMENT (of the abstract entered in Block 20, if different from Report)

18. SUPPLEMENTARY NOTES

19. KEY WORDS (Continue on reverse side if necessary and identify by block number)

Nucleation
Carbon Gas
Agglomeration
Carbon Particles
Carbon Three
Carbon Two

20. ABSTRACT (Continue on reverse side if necessary and identify by block number)

The specific approach taken in this work was to study particle formation in a cooling jet of carbon vapor diluted by an inert carrier gas. Vapor was produced by the evaporation of a resistance heated graphite tube. The carbon vapor, mixed with carrier gas, flowed into a light scattering chamber where spectroscopic measurements were used to monitor concentrations of molecular species. Particles were also collected for electron microscopy. An initial reaction leading to particle formation was identified as $C_2 + C_3 \rightarrow C_5$ with a gas kinetic rate. Particulates were found to be spherical, of approximately equal diameter and frequently chained in the manner of hydrocarbon soot.

DD FORM 1 JAN 73 1473 EDITION OF 1 NOV 65 IS OBSOLETE

UNCLASSIFIED